Cell Cycle 14:4, 566–576; February 15, 2015; © 2015 Taylor & Francis Group, LLC

S-phase-dependent p50/NF-κB1 phosphorylation in response to ATR and replication stress acts to maintain genomic stability

Clayton D Crawley[1], Shijun Kang[1], Giovanna M Bernal[1], Joshua S Wahlstrom[1], David J Voce[1], Kirk E Cahill[1], Andrea Garofalo[1], David R Raleigh[1], Ralph R Weichselbaum[2], and Bakhtiar Yamini[1,*]

[1]Department of Surgery, Section of Neurosurgery; The University of Chicago; Chicago, IL USA; [2]Department of Radiation and Cellular Oncology; The Ludwig Center for Metastasis Research; The University of Chicago; Chicago, IL USA

Keywords: ATR, DNA damage, NF-κB, p50, replication stress, S-phase

Abbreviations: ATM, ataxia telangiectasia mutated; ATR, ataxia telangiectasia mutated and Rad3-related; Bax, BCL2-associated X protein; Bclxl, Bcl-2-like protein; ChIP, chromatin immunoprecipitation; Chk1, checkpoint kinase 1; DSBs, double-strand breaks; H2AX, histone 2AX; HR, homologous recombination; Hu, hydroxyurea; IκB, inhibitor kappaB; IκK, inhibitor kappaB kinase; IR, ionizing radiation; NF-κB, nuclear factor-kappaB; RS, replication stress; RT-PCR, reverse transcriptase polymerase chain reaction; siRNA, short interfering RNA; TAM, tamoxifen; TMZ, temozolomide; TopBP1, topoisomerase-binding protein-1.

The apical damage kinase, ATR, is activated by replication stress (RS) both in response to DNA damage and during normal S-phase. Loss of function studies indicates that ATR acts to stabilize replication forks, block cell cycle progression and promote replication restart. Although checkpoint failure and replication fork collapse can result in cell death, no direct cytotoxic pathway downstream of ATR has previously been described. Here, we show that ATR directly reduces survival by inducing phosphorylation of the p50 (NF-κB1, p105) subunit of NF-κB and moreover, that this response is necessary for genome maintenance independent of checkpoint activity. Cell free and in vivo studies demonstrate that RS induces phosphorylation of p50 in an ATR-dependent but DNA damage-independent manner that acts to modulate NF-κB activity without affecting p50/p65 nuclear translocation. This response, evident in human and murine cells, occurs not only in response to exogenous RS but also during the unperturbed S-phase. Functionally, the p50 response results in inhibition of anti-apoptotic gene expression that acts to sensitize cells to DNA strand breaks independent of damage repair. Ultimately, loss of this pathway causes genomic instability due to the accumulation of chromosomal breaks. Together, the data indicate that during S-phase ATR acts via p50 to ensure that cells with elevated levels of replication-associated DNA damage are eliminated.

Introduction

During the normal cell cycle, endogenous or acquired impediments to DNA replication result in the appearance of stretches of single-stranded DNA, or single-strand/double-strand DNA junctions, that are the basic substrate of replication stress (RS).[1,2] To modulate the genotoxic effects of RS, cells induce a checkpoint response coordinated by the apical damage kinase, ATR.[3] ATR is activated following the co-localization of a series of proteins including the critical co-activator, topoisomerase-binding protein-1 (TopBP1), a protein that contains an activation domain that is able to induce ATR on its own.[4,5] Although the ATR response attenuates the amount of DNA double-strand breaks (DSBs) that accumulate as a result of RS,[6] low levels of strand breaks are often tolerated, possibly because DSB repair is inefficient below a certain threshold.[7] In order to prevent the propagation of such potentially harmful damage, multi-cellular species activate a variety of pathways that eliminate cells with raised levels of DNA damage.

The transcription factor NF-κB plays a pivotal role in modulating the response to DNA damage.[8] While genotoxic stress activates NF-κB by a well-described mechanism involving DNA DSBs and ATM,[9] the response of NF-κB to ATR and RS is poorly understood. Preliminary data suggest that ATR can inhibit NF-κB,[10,11] yet the full mechanism and physiological role of this pathway is unclear. NF-κB proteins are composed of 5 subunits: p50 (NF-κB1, p105), p52 (NF-κB2, p100), p65 (relA), c-rel, and relB that bind to DNA as dimers and are retained in the cytoplasm through interaction with inhibitor-κB (IκB) proteins.[12] Although the NF-κB system is generally regarded as a stimulus-induced transcription factor, significant levels of DNA bound NF-κB dimers are found in resting cells. The most abundant form of DNA bound NF-κB in unstimulated cells consists of the p50/p65 heterodimer. Interestingly,

*Correspondence to: Bakhtiar Yamini; Email:byamini@surgery.bsd.uchicago.edu
Submitted: 03/14/2014; Revised: 11/17/2014; Accepted: 11/20/2014
http://dx.doi.org/10.4161/15384101.2014.991166

during the unperturbed cell cycle, a complex exchange of NF-κB dimers and subunit post-translational modifications occur,[13] suggesting that NF-κB proteins likely play a fundamental role in the basal homeostatic process.

We recently reported that certain DNA damaging agents inhibit NF-κB by inducing Chk1-mediated phosphorylation of p50 Ser329.[14] Given the association between ATR/Chk1 and RS, we set out to examine the role of p50 in response to RS. Our results demonstrate that ATR inhibits NF-κB and induces p50 phosphorylation in response to RS. Moreover, this pathway is induced during S-phase and acts to maintain cellular genome stability by facilitating elimination of damaged cells.

Results

Replication stress inhibits NF-κB DNA binding in an ATR- and p50-dependent manner

To examine NF-κB in the setting of RS, cells were administered the ribonucleotide reductase inhibitor, hydroxyurea (Hu), and NF-κB examined by gel shift assay. As previously reported,[10] Hu activates NF-κB in $ATM^{+/+}$ cells (**Fig. 1A**). However, in the absence of ATM, we note that Hu not only fails to induce but actually inhibits NF-κB within about 1 hour of treatment (**Fig. 1A; Fig. S1A**). Supershift analysis demonstrates that the NF-κB dimer in these cells is comprised of p50 and p65 (**Fig. S1B**). While anti-p50 and anti-p65 antibodies do not result in a discernable supershifted band, they break up the NF-κB-DNA complex, an observation not seen with a non-specific control antibody. In addition, in the absence of ATM, other genotoxic agents that induce RS, including aphidicolin and etoposide, also inhibit NF-κB (**Fig. S1C**). Inhibition of NF-κB by RS is blocked by caffeine, a general ATM/ATR inhibitor (data not shown). Therefore, to examine whether ATR specifically is involved in the inhibition of NF-κB, ATR was depleted using siRNA. Loss of ATR blocks the ability of Hu to inhibit NF-κB (**Fig. 1B**). Moreover, siRNA studies also demonstrate that p50 is required for inhibition of NF-κB by RS (**Fig. 1B**). Importantly, the inhibition of NF-κB is independent of changes in either IκBα protein level or nuclear p50 and p65 levels (**Fig. 1C**) suggesting that RS and ATR specifically affect NF-κB DNA binding and not nuclear translocation. Consistent with the ability of RS to activate Chk1, a previously identified p50 S329 kinase,[14] Hu induces S329-phosphorylation with kinetics similar to the inhibition of NF-κB DNA binding (**Fig. 1C**). The inhibition of DNA binding by Hu is reflected by a decrease in NF-κB transcriptional activity, as measured using a reporter bearing 3 repeats of the immunoglobulin κ-light chain κB-site, a finding also noted to be ATR- and p50-dependent (**Fig. 1D**).

As chemotherapeutics like Hu have pleotropic effects and also induce DNA DSBs, we next sought to examine NF-κB in response to a non-chemotherapeutic model of RS. Synthetic poly $(dA)_{70}$-poly$(dT)_{70}$ oligonucleotides (TA oligos) that form the minimal replicative intermediates previously used to study RS signaling in Xenopus and mammalian cell extracts[15,16] were obtained and used *in vitro*. Nuclear extracts were isolated from U87 human glioma cells that have stably-suppressed endogenous p105,[14] the parental protein of p50. Extracts were supplemented with purified $p50^{WT}$ or $p50^{S329A}$, a mutant that cannot be phosphorylated by Chk1. As initially noted using these oligos,[15,16] TA but not monomeric poly$(dT)_{70}$ oligonucleotides (T oligos) activate Chk1 by phosphorylation (**Fig. 2A**). Moreover, consistent with the findings using Hu, we find that TA oligos both induce p50 S329 phosphorylation and inhibit NF-κB binding in a p50-S329-dependent fashion (**Fig. 2A**). These responses are abrogated by caffeine and the Chk1 inhibitor, Gö6976, but not by IκK inhibition (**Fig. 2A**). In these cells, the NF-κB dimer is comprised of p50/p65 as shown by supershift analysis (**Fig. S2A**). The requirement of ATR for inhibition of NF-κB by TA oligos is demonstrated using extracts from cells expressing wildtype, or kinase-dead, ATR,[17] and the role of Chk1 is shown using Gö6976 (**Fig. 2B**). In addition, studies using living, immortal *Nfkb1*$^{-/-}$ MEFs stably expressing $p50^{WT}$ or $p50^{S329A}$ transfected with the oligos recapitulate the cell-free experiments (**Fig. S2B**) and also demonstrate that TA oligos inhibit NF-κB transcriptional activity in a manner dependent on p50 S329 (**Fig. S2C**). Importantly, the $p50^{S329A}$ mutant binds DNA (**Fig. S2D**), and hetero-dimerizes with p65 as efficiently as $p50^{WT}$ (**Fig. S2E**). Consistent with the latter observation, the primary NF-κB dimer in stable *Nfkb1*$^{-/-}$ MEFs expressing $p50^{WT}$ or $p50^{S329A}$ is made of p50/p65 (**Fig. S2F**). These results support the findings with pharmacological RS-inducing agents and indicate that RS inhibits NF-κB in an ATR-dependent manner.

ATR inhibits NF-κB activity in the absence of DNA damage

While TA oligos simulate replication forks and activate ATR, these oligos can also induce ATM and have primarily been used for *in vitro* studies.[18] Therefore, to more specifically induce ATR and examine NF-κB *in vivo*, a tamoxifen (TAM)-inducible system that incorporates the activation domain of TopBP1 fused to the estrogen receptor ($TopBP1^{ER}$) was used.[5] Importantly, this system allows ATR induction in the absence of DNA DSBs and without activation of ATM.[5] Exposure of 293T cells stably expressing $TopBP1^{ER}$ to TAM leads to activation (phosphorylation) of ATR within 30 minutes (**Fig. 3A**). This response subsequently results in p50 S329 phosphorylation and inhibition of NF-κB binding, both of which occur in an ATR- and Chk1-dependent manner as demonstrated using ATR-specific siRNA and Chk1 inhibitor (**Fig. 3A; Fig. S3A**). Again, the basal, NF-κB dimer present in these cells is comprised of p50 and p65, as demonstrated by supershift analysis (**Fig. S3B**). Neither TAM in the absence of $TopBP1^{ER}$ nor $TopBP1^{ER}$ alone result in inhibition of NF-κB (**Fig. S3C**). Exposure to TAM also leads to inhibition of NF-κB transcriptional activity in a manner dependent upon ATR and p50 (**Fig. 3B**). Subsequently, to examine the role of S329 in this pathway, *Nfkb1*$^{-/-}$ MEFs stably expressing $p50^{WT}$ or $p50^{S329A}$ were infected with a retrovirus expressing $TopBP1^{ER}$. Administration of TAM to these cells leads to inhibition of NF-κB DNA binding, and transcriptional activity, specifically in a p50 S329-dependent manner (**Fig. 3C; Fig. S3D**). To examine whether the effect on NF-κB is reflected by a change in endogenous gene expression, we examined the NF-κB-regulated

anti-apoptotic gene, *BCLXL*, whose inhibition is required for cytotoxicity by S-phase specific alkylating agents.[19] As we previously noted, this gene has p50/p65 heterodimers bound to its promoter at baseline.[14,20] In both human and murine cells, ATR induced by Top-BP1^{ER} leads to a decrease in *BCLXL* expression, a finding that is specifically dependent on p50 S329 (**Fig. 3D; Fig. S3E**). Of note, TAM inhibits NF-κB trans-activity in the absence of p65, as seen using *P65*$^{-/-}$ MEFs (**Fig. S3F**). Also, *BCLXL* mRNA expression can still be inhibited by ATR in human cells depleted of p65 with si-RNA (**Fig. S3G**). Interestingly, despite inhibition of NF-κB activity and *Bclxl* mRNA expression, activation of ATR in the absence of additional DNA damage does not affect overall clonal survival (**Fig. S3H**).

In sum, the data generated using both *in vivo* and cell free systems, demonstrate that the ATR response to RS leads to inhibition of NF-κB p50/p65 DNA binding and NF-κB transcriptional activity that is dependent on p50-S329.

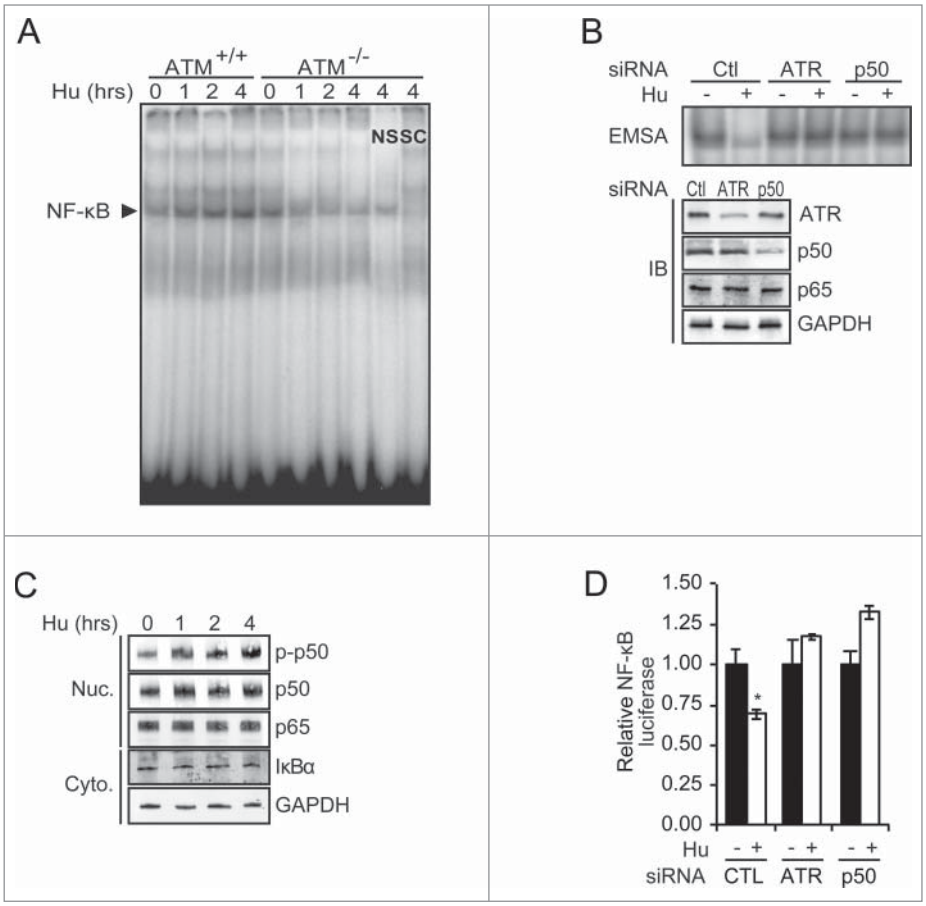

Figure 1. RS inhibits NF-κB in an ATR- and p50-dependent manner. (**A**) Human ATM$^{-/-}$ and ATM$^{+/+}$ cells were treated with Hu (2 mM) and EMSA performed after isolation of nuclear extracts. Competition was performed with specific (SC) and non-specific (NS) cold DNA. (**B**) NF-κB EMSA (upper) and immunoblot (IB, lower) using nuclear extract from ATM$^{-/-}$ cells transfected with the indicated siRNA and treated with Hu (2 mM, 4 hrs). (**C**) IB in nuclear and cytoplasmic fractions from ATM$^{-/-}$ cells treated with Hu (2 mM) (p-p50: anti-phospho-S329-p50 antibody). (**D**) NF-κB-dependent luciferase assay in ATM$^{-/-}$ cells transfected with siRNA and treated with vehicle or 2 mM Hu (4 hrs). Data show mean value relative to *renilla*, normalized to control, ± SD of triplicate samples. *$P < 0.05$ relative to untreated.

p50 S329 phosphorylation occurs during S-phase and enables inhibition of NF-κB

ATR is activated during the unperturbed S-phase,[21,22] therefore, we examined whether NF-κB and p50 are also modified at this time. U87 glioma cells were synchronized at G2/M using nocodazole and nuclear extracts isolated at the indicated times following release (**Fig. 4A**). Maximal p50 S329-phosphorylation occurs when the greatest percentage of cells are in S-phase, identified by FACS analysis and cyclin E expression to be approximately 12 hours after release from synchronization (**Fig. 4A**). Moreover, EMSA reveals that it is during this phase that NF-κB DNA binding is at its lowest level (**Fig. 4A**, lower blot). As we previously noted, in these glioma cells NF-κB dimers are comprised of p50 and p65.[14] Similarly, following synchronization of cells at G1 by double thymidine block, NF-κB DNA binding is also noted to nadir during S-phase, indicating that the NF-κB changes are not merely a consequence of the synchronization method (**Fig. 4B**). Moreover, the reduced DNA binding during S-phase is Chk1- and caffeine-dependent (**Fig. 4B**). Consistent with the finding that ATR inhibits *BCLXL* expression, S-phase-dependent p50 phosphorylation and reduced DNA binding is mirrored by a decrease in p50 recruitment to the *BCLXL* promoter at this time (**Fig. 4C**). Furthermore, *BCLXL* mRNA expression is also attenuated at this time (**Fig. 4D**), ultimately leading to a modest but reproducible decrease in Bclxl protein expression in late S-phase (**Figs. 4A and E**). To investigate the role of p50 S329 in the cell cycle-dependent regulation of NF-κB, *Nfkb1*$^{-/-}$ MEFs stably expressing p50^{WT} or p50^{S329A} were synchronized by thymidine block and examined following release. As with human cells, p50 phosphorylation and the nadir of NF-κB DNA binding occur specifically during S-phase (**Fig. 4F**), findings that are blocked by mutation of S329. Similarly, the S-phase-dependent decrease in *Bclxl* mRNA expression is blocked by S329 mutation (**Fig. S4A**). Together, these results demonstrate that p50 is phosphorylated during S-phase resulting in an S329-dependent decrease in NF-κB DNA binding and Bclxl expression.

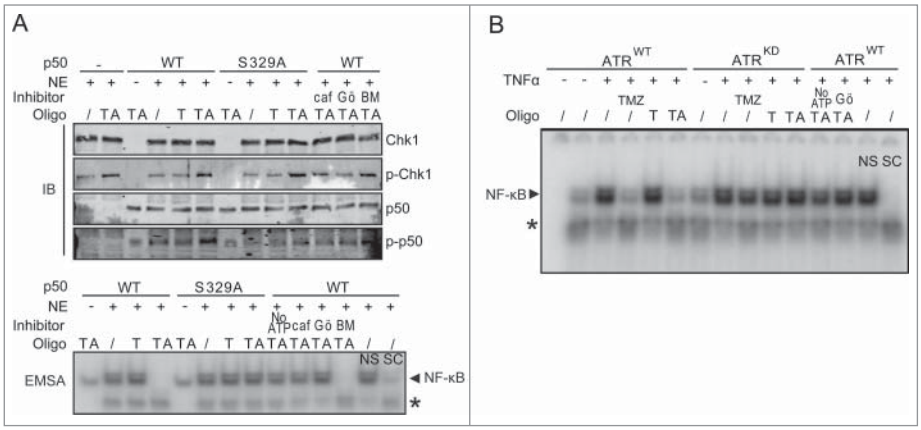

Figure 2. Oligonucleotide mimetics of RS inhibit NF-κB DNA binding in a p50 S329-dependent manner. (**A**) Nuclear extract (NE) isolated from U87-sh-p105 cells were supplemented with bacterially expressed $p50^{WT}$ or $p50^{S329A}$ (or no p50). IB (upper) or EMSA (lower) was performed following stimulation of extract with TA or T oligos under kinase conditions. Extracts were supplemented with caf-caffeine (0.5 mM); Gö- Gö6976 (1 μM) or BM-BMS-345541 (IKK inhibitor) (1 μM) where shown. p-Chk1: anti-phospho-Ser345 Chk1. Specific (SC) and non-specific (NS) competitor. * Non-specific band present in nuclear extract. (**B**) NE was isolated from vehicle or TNFα-stimulated (10 ng/ml, 30 min) U2OS cells stably expressing tet-on wild-type ATR (ATR^{WT}) or kinase-dead ATR (ATR^{KD}) 48 hrs after stimulation with 1 mg/ml doxycycline. EMSA was performed after incubation of extract with TA or T oligos (or vehicle). EMSA was also run following treatment of cells with TMZ (100 μM, 16 hrs, lanes 4 and 9). Controls were also performed in the presence of Gö- Gö6976, in the absence of ATP or with cold competitors as shown. *Non-specific band.

anti-apoptotic gene expression, it is possible that the ATR-mediated checkpoint or damage repair response also contribute to modulating survival. However, the observation that *Nfkb1*$^{-/-}$ MEFs stably expressing p50 constructs cycle at similar rates (**Fig. 5B, inset**) and have similar percentages of cells in S-phase (**Fig. 5C**) indicates that p50 phosphorylation does not affect the replication checkpoint. With regard to strand break repair, homologous recombination (HR), the major DSB repair pathway associated with replication,[23] is unaffected by either loss or mutation of p50 (**Fig. 5D; Fig. S4B**). In addition, the finding that IR induces similar levels of breaks in $p50^{WT}$ and $p50^{S329A}$-expressing cells (**Fig. S4C**), suggests that p50 phosphorylation does not affect other pathways that act to repair DSBs. Taken together, these data indicate that in response to ATR, p50 sensitizes cells to DNA strand breaks by a mechanism independent of checkpoint or damage repair and that this pathway is functional during S-phase.

p50 phosphorylation during S-phase sensitizes cells to DNA strand breaks independent of damage repair

It was previously noted that p50 signaling sensitizes cells to cytotoxicity in response to DNA damaging agents.[14] We therefore examined whether this pathway also acts downstream of ATR to modulate survival during the cell cycle. First, *Nfkb1*$^{-/-}$ MEFs expressing $TopBP1^{ER}$ and either $p50^{WT}$ or $p50^{S329A}$ were exposed to TAM, to induce ATR signaling, and also to 0.5 Gy ionizing radiation (IR), to induce low levels of DNA strand breaks. As $TopBP1^{ER}$ activation does not induce appreciable levels of DNA damage,[5] IR delivery can be used to induce strand breaks at a specific time. IR was administered either 8 hours before or after exposure to TAM. Importantly, activation of ATR for 8 hours is sufficient to induce p50-signaling but does not alter cell survival (**Fig. 3; Fig. S3F**). A decrease in survival is noted when the p50 is activated prior to IR, compared to the reverse, and specifically in cells expressing $p50^{WT}$ but not $p50^{S329A}$ (**Fig. 5A**) suggesting that p50 phosphorylation sensitizes cells to DNA strand breaks. To examine whether p50 phosphorylation in S-phase mediates a similar effect, *Nfkb1*$^{-/-}$ MEFs stably expressing $p50^{WT}$ or $p50^{S329A}$ were synchronized by thymidine block and then treated at the indicated time following release with low dose IR. Despite the minor levels of damage induced by 0.5 Gy IR, a significant decrease in surviving fraction is noted in cells expressing $p50^{WT}$ and specifically at the time when p50 is phosphorylated (**Fig. 5B**). Together, these results indicate that p50 phosphorylation in response to ATR sensitizes cells to DNA damage during S-phase.

Although the data suggest that the mechanism of sensitization to strand breaks occurs via ATR/p50-induced inhibition of

Phosphorylation of p50 is necessary for maintaining genome stability

If cell cycle-dependent p50 phosphorylation plays a physiological role in sensitizing to damage, then loss of this response in proliferating cells would be expected to result in damage accumulation. To examine this hypothesis, freshly isolated primary *Nfkb1*$^{-/-}$ MEFs were infected with p50 constructs and DNA DSB levels assessed following serial passage by analysis of γ-H2AX focus formation. The percentage of γ-H2AX-positive cells rises with increasing passage and expression of $p50^{WT}$ significantly reduces the increase relative to empty vector (**Fig. 6A; Fig. S5**). The observation that cells expressing $p50^{S329A}$ have higher endogenous γ-H2AX foci than $p50^{WT}$ cells indicates that p50 phosphorylation is necessary to attenuate spontaneous replication associated damage build up. Given the well-described association between DNA damage accumulation and senescence,[24] we examined senescence in serially passaged primary MEFs. *Nfkb1*$^{-/-}$ MEFs expressing $p50^{S329A}$ have a significantly higher level of β-galactosidase staining at late passage than isogenic cells expressing $p50^{WT}$ (**Fig. 6B**). These data suggest that p50 phosphorylation is required to maintain genomic stability. To directly examine genome integrity, metaphase spreads were studied in MEFs infected with the p50 constructs. Despite initially having equivalent levels of DNA breaks and gaps, primary *Nfkb1*$^{-/-}$ MEFs expressing $p50^{WT}$ accumulate significantly less breaks and gaps than $p50^{S329A}$-expressing cells following serial passage (**Fig. 6C**). These findings demonstrate that p50 phosphorylation is necessary to attenuate spontaneous DNA damage accumulation and to maintain genomic integrity.

Discussion

In this report, we demonstrate that RS, induced either pharmacologically or by oligonucleotide fork mimetics, causes phosphorylation of p50 and inhibition NF-κB activity. This response is shown to require the damage kinase ATR and, in contrast to the activation of NF-κB by DNA DSBs, is independent of ATM. A previous report noted a propensity of ATR to block NF-κB and suggested that ATR acts in opposition to ATM to block NF-κB nuclear translocation by inhibiting inhibitor-κB kinase (IκK).[10] While our work also shows that ATR inhibits NF-κB, we demonstrate that ATR acts on nuclear p50-containing NF-κB dimers to modulate NF-κB activity independent of IκBα. Interestingly, in response to $p14^{ARF}$, ATR was also reported to inhibit NF-κB activity in an IκBα-independent fashion by inducing phosphorylation of p65 T505.[11] Although we note that inhibition of NF-κB activity by ATR can occur even in the absence of p65, given that c-rel cross-compensates when p65 is lost,[25] it is likely that in the physiological setting p65-dependent signaling is also required for the ATR response. Taken together, these previous studies and ours indicate that the ATR pathway incorporates several mechanisms to modulate NF-κB signaling and moreover, that this occurs in a promoter-specific manner. Most importantly, these studies arrive at the same conclusion, namely, that the functional role of the NF-κB response to ATR acts to decrease survival and promote cell death (**Fig.** 7).

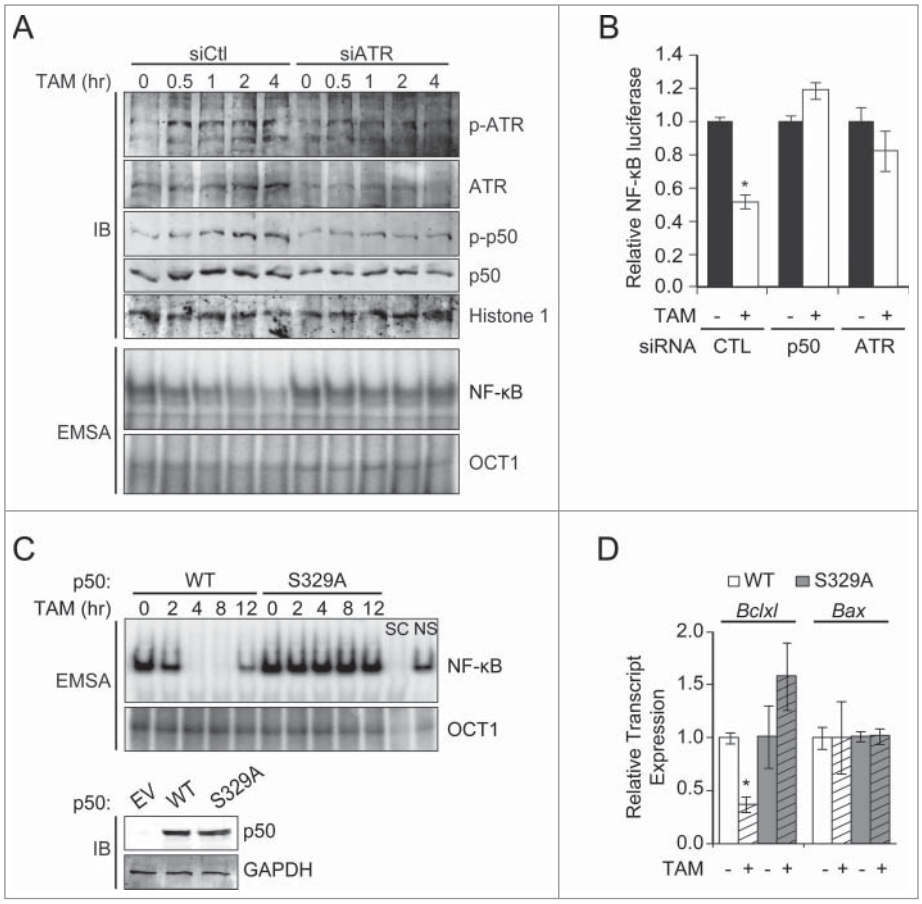

Figure 3. ATR inhibits NF-κB activity independent of DNA damage. (**A**) 293T cells stably expressing $TopBP1^{ER}$ were transfected with the indicated siRNA and stimulated with TAM (500 nM). IB and EMSA (NF-κB and Oct1) were performed on nuclear extracts isolated at the indicated time. p-ATR (anti-phospho-Ser428 ATR). (**B**) NF-κB-dependent luciferase assay in 293T-$TopBP1^{ER}$ cells expressing the indicated siRNA following stimulation with TAM (8 hrs). *$P < 0.01$. (**C**) *Nfkb1*$^{-/-}$ MEFs stably expressing $p50^{WT}$ or $p50^{S329A}$ were infected with $TopBP1^{ER}$ and stimulated with TAM (500 nM). EMSA was performed on nuclear extracts using the indicated probe. IB shows equal p50 expression in cells. (**D**) qPCR of *Bclxl* and *Bax* mRNA expression in cells from (C) following stimulation with TAM (8 hrs). Data show mean normalized value, ± SEM of triplicate samples from 3 experiments. *$P < 0.05$ relative to untreated.

Our data indicate that the p50-mediated response to ATR, while not sufficient on its own to induce cytotoxicity, facilitates loss of survival by enabling inhibition of anti-apoptotic gene expression. These findings, coupled with the observation that ATR is activated and p50 phosphorylated during replication, suggest that p50 acts during S-phase to facilitate death of damaged cells. Consistent with this hypothesis, we note that loss of the p50 signaling due to S329 mutation, results in an increase in the accumulation of cells with DNA breaks. These data suggest a model in which ATR activation during S-phase induces a pathway separate from the checkpoint that acts on p50 to modulate NF-κB activity and facilitate cell elimination (**Fig.** 7). In the presence of normal p50 signaling, cells that acquire elevated levels of DNA strand breaks (i.e. levels that are harmful to the genome) are removed from the population. In the absence of p50, the cytotoxic threshold is raised resulting in DNA damage tolerance and genomic instability. Importantly, if replication-associated damage is adequately addressed, then p50-mediated signaling has no deleterious effects and the cell continues to cycle. This last point is emphasized by the observation that the p50 response, involving a decrease in Bclxl expression, while significant, is small and not great enough in magnitude to affect survival in the absence of additional damage.

It is recognized that during S-phase ATR functions to stabilize replication forks and coordinate the checkpoint response to ensure faithful DNA replication prior to mitosis.[3,26] However, if the overall role of ATR is to maintain genomic stability,[27] it is likely that this master-regulator of the RS response would directly modulate survival in the event that replication-induced damage is not adequately repaired. Such a direct ATR-induced cytotoxic pathway, independent of the checkpoint, has not been previously

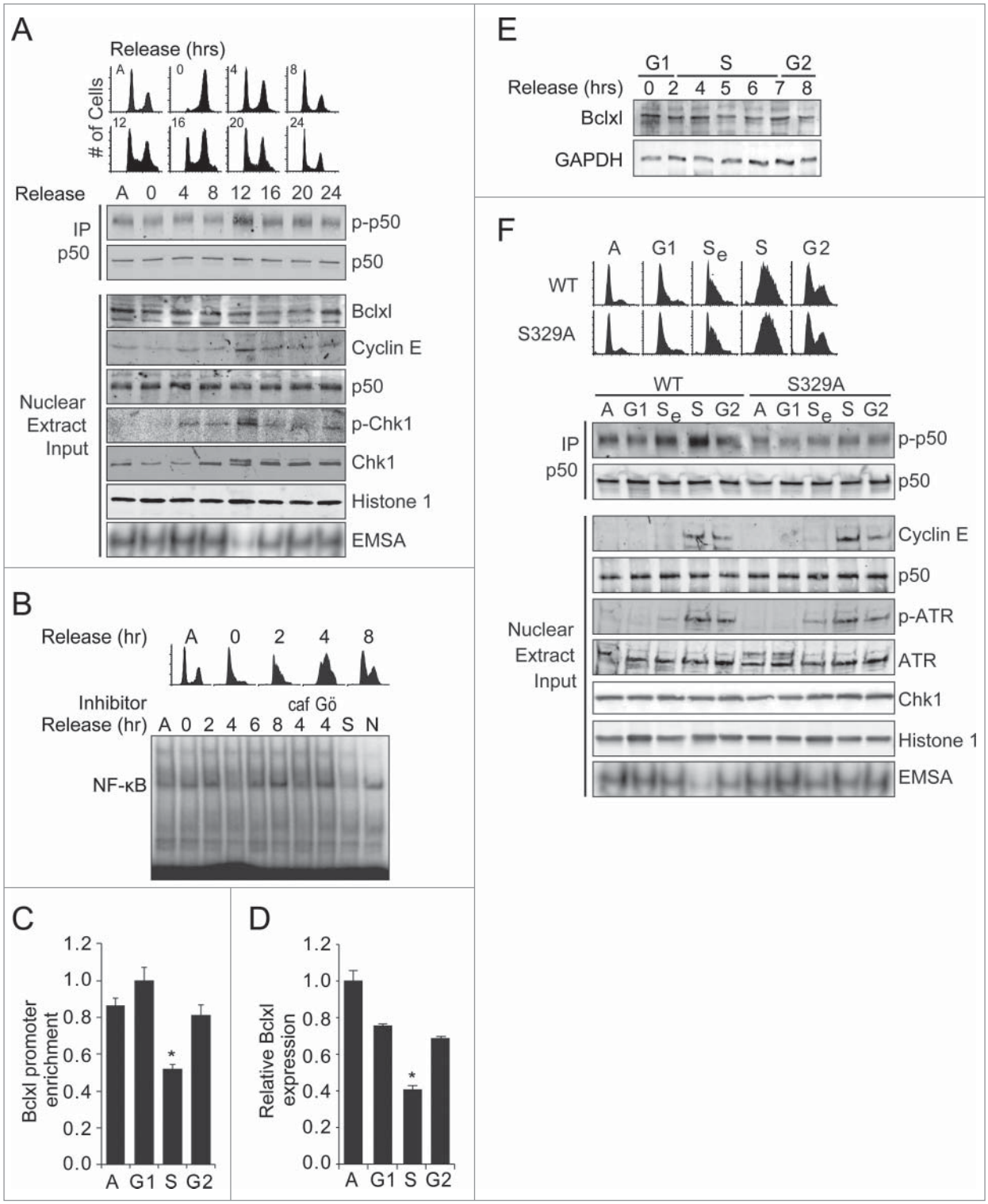

Figure 4. p50 is phosphorylated and NF-κB binding inhibited during S-phase. (**A**) U87 glioma cells were released from nocodazole synchronization, nuclear lysates isolated and IB performed on lysate or following IP. NF-κB EMSA (lower blot) was also performed. Cell cycle phase at the corresponding time following release is shown above. Asynchronous (A). (**B**) U87 cells were released from thymidine block and EMSA performed following isolation of nuclear lysates. Cells were pre-incubated with caffeine (0.5 mM) and Gö6976 (1 μM) where shown. (**C**) qChIP in U87 cells at the indicated phase following thymidine release. Data show enrichment of p50 relative to IgG, histone H1 and input, ± SEM of 3 separate experiments. *$P < 0.03$ relative to A. (**D**) qPCR of *BCLXL* mRNA in U87 cells at the indicated phase. Mean ± SEM of triplicate samples from 3 separate experiments. *$P < 0.05$ relative to G1. (**E**) IB with anti-Bclxl antibody in U87 cells following release from thymidine. (**F**) *Nfkb1*$^{-/-}$MEFs stably expressing p50^{WT} or p50^{S329A} were released from thymidine block, nuclear lysates isolated and IB performed on lysate or following IP. NF-κB EMSA (lower blot) was performed using the same samples. S_e- early S-phase. Images are representative of 2 or 3 separate experiments.

reported firstly because ATR is an essential gene that plays a dominant role in modulating the checkpoint,[28-31] as do downstream mediators of cytotoxicity, such as p53;[32] and secondly because yeast, the organism in which much of the information on ATR/Mec1 has been obtained,[33-35] is unicellular and lacks NF-κB.

Given the imperfect nature of DSB repair,[36] even a slight rise in DNA DSB levels can lead to increased mutation formation and tissue dysfunction. The p50/NF-κB response to RS can be considered a pathway that addresses the minor levels of damage encountered during replication. p50 is ideally situated to modulate the response to RS not only because it is found in virtually all tissues, but also because it constitutes a primary DNA-bound NF-κB subunit that is present at baseline. Importantly, as DNA-bound p50 can be modified quickly, in comparison to latent NF-κB pools that must first translocate to the nucleus, it can relatively rapidly mediate signaling during replication. Although NF-κB is best known as a stimulus-induced transcription factor, the presence of basal activity suggests that NF-κB also contributes to more routine cellular processes. Consistent with a role in regulating low endogenous damage levels, loss of p50/*Nfkb1* does not lead to overwhelming damage accumulation or embryonic lethality;[37] however, loss of this subunit does result in chronic disease as demonstrated by the propensity of *Nfkb1*$^{-/-}$ mice to develop premature age-related findings (see refs. 38– 40 and unpublished data, BY).

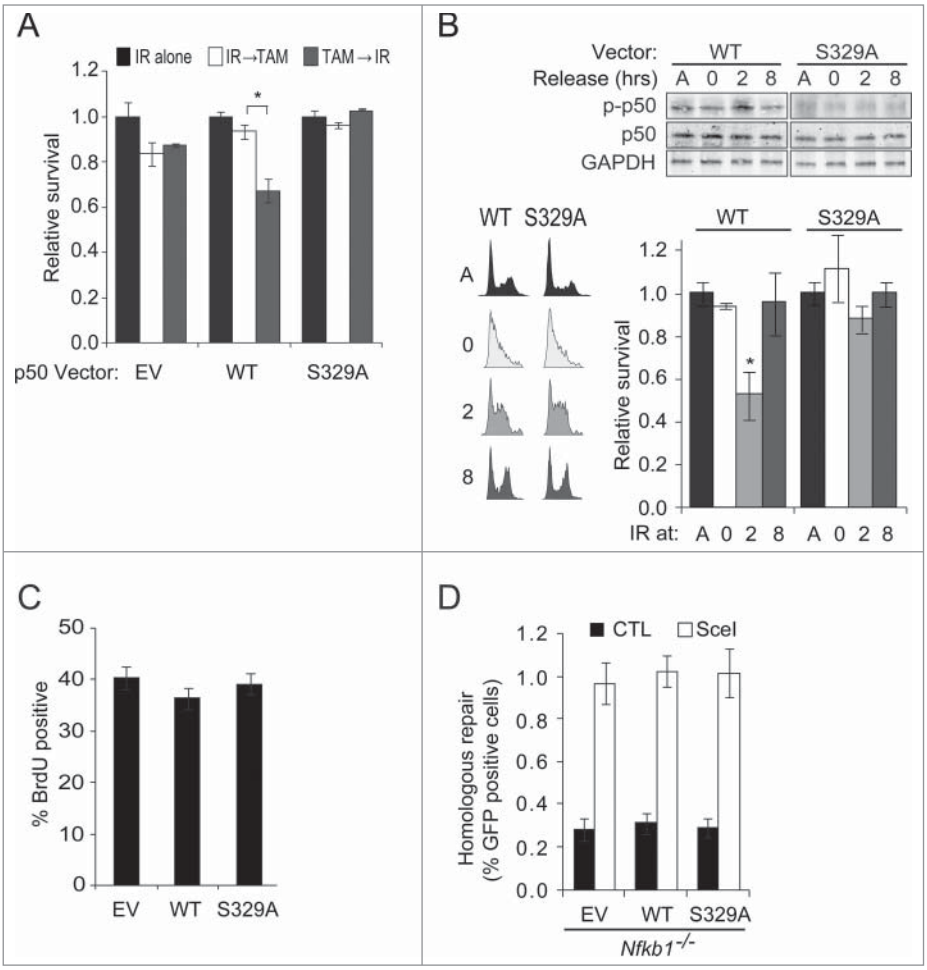

Figure 5. p50 phosphorylation in response to ATR sensitizes cells to DNA strand breaks. (**A** and **B**) Clonogenic assays. (**A**) *Nfkb1*$^{-/-}$MEFs expressing TopBP1^{ER} and the p50 vector shown were exposed to 0.5 Gy IR and TAM, in the order indicated, separated by 8 hrs. Inset: IB showing p50 expression. Data is normalized to IR alone, ± SEM of duplicate samples from 3 experiments (TAM alone does not alter survival). *$P < 0.02$. (**B**) Thymidine synchronized *Nfkb1*$^{-/-}$MEFs stably expressing p50^{WT} or p50^{S329A} were exposed to 0.5 Gy IR at indicated time following release. A- asynchronous cells. IB of nuclear lysates (upper) and FACS analysis (left) from the same experiment is shown (anti-p50 IB in asynchronous shows equal p50 expression). *$P < 0.02$, relative to p50^{S329A}. (**C**) FACS analysis of BrdU labeling in asynchronous *Nfkb1*$^{-/-}$MEFs expressing empty vector, p50^{WT} or p50^{S329A}. Mean ± SD of triplicate samples from 3 experiments shown. n ≥ 10^5 cells per group. (**D**) HR assay in *Nfkb1*$^{-/-}$MEFs stably expressing empty vector (EV), p50^{WT} or p50^{S329A} following co-transfection with DR-GFP and either control vector (CAG) or pC⇓ASce (SceI). Data show value ± SD of triplicate samples (n = 3000– 5000 cells per group).

In summary, we propose that p50-signaling acts as a fail-safe mechanism by which ATR ensures that cells with raised levels of DNA damage do not survive. Ultimately, this response functions in multicellular species to maintain overall organismal health at the expense of individual cellular integrity.

Materials and Methods

Antibodies, reagents and plasmids

Cellular lysates were subjected to SDS-PAGE and western blotting performed as described.[20] The antibodies used include: anti-p50 (Santa Cruz, sc7178 and sc8414); anti-phospho-S329-p50 (YenZym Antibodies, San Francisco, CA);[14] anti-ATR and anti-phospho-S428-ATR (Cell Signaling, 2790 and 2853, respectively); anti-p65 (Santa Cruz, sc-8008); anti-IkBα (Cell Signaling, 9242); anti-Flag (Cell Signaling, 2368); anti-Chk1 and anti-phospho-S345-Chk1 (Cell Signaling, 2345 and 2341s, respectively); anti-histone 1 (Santa Cruz; sc-8030); anti-Gapdh (Santa Cruz, sc-137179); anti-Bclxl (Cell Signaling, 2762); anti-cyclin E (Santa Cruz, sc-198); anti-phospho-S140-H2AX (Cell Signaling, 9718). Hydroxyurea, tamoxifen, caffeine, Gö6976, BMS-345541, TNFα, etoposide, thymidine, nocodazole, aphidicolin and cyclohexamide were obtained from Sigma. TMZ was obtained from the Drug Synthesis and Chemistry Branch,

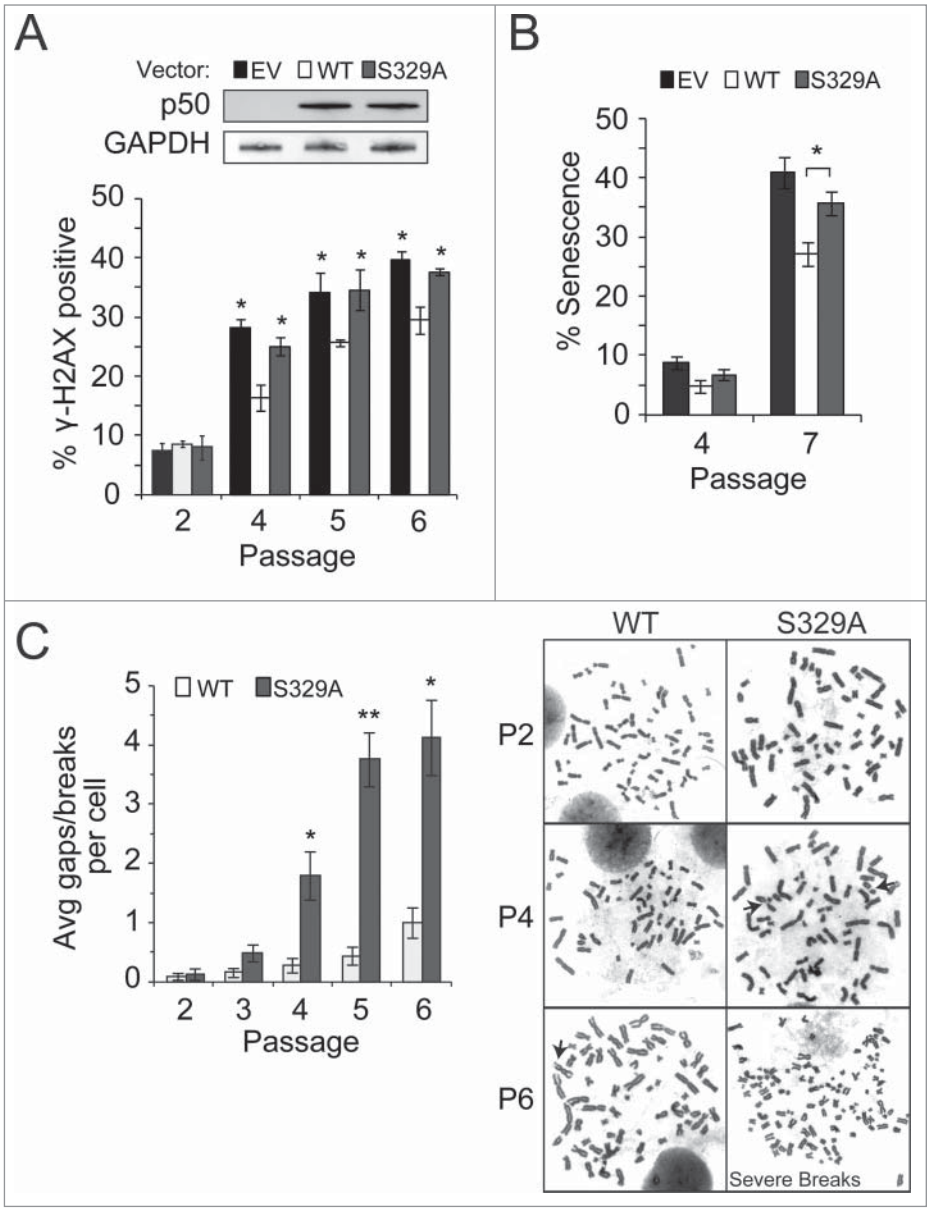

Figure 6. p50 S329 is necessary to maintain genome stability. (**A**–**C**) Primary *Nfkb1*$^{-/-}$MEFs were infected at passage 1 with the indicated p50 construct and analyses made after serial passage. Experiments were performed using at least 3 separate MEF isolations/ infections expressing equivalent levels of p50. (**A**) γH2AX foci. *$P < 0.001$ relative to p50^{WT}-expressing cells. Inset: IB with anti-p50. Data from (**A** and **B**) show mean ± SD (n ≥ 150 cells). (**B**) β-gal staining. *$P < 0.005$. (**C**) Spontaneous breaks and gaps. n = 25 metaphase spreads per sample. Data show mean ± SEM. *$P < 0.005$ relative to p50^{WT}-expressing cells. Representative metaphase spreads shown (right). Arrows indicate chromosomal gaps/breaks. P6 cells expressing p50^{S329A} have multiple/severe breaks.

Developmental Therapeutics Program, National Cancer Institute, NIH. TMZ was dissolved in DMSO (final concentration <0.1% v/v). The TopBP1^{ER} construct was a generous gift from Dr. Oscar Fernandez-Capetillo.

To create p50 retroviral constructs, p50 was liberated from pcDNA3.1-p50 previously described,[20] by digesting with PmeI and XhoI and ligated into the BglII site of pMSCV-MigR1 containing an IRES-GFP insert. The QuikChange Lightning Site Directed Mutagenesis Kit (Stratagene) was used to create individual site mutants in the MigR1-p50 backbone.

Cells, RNA interference and retroviral infection

Experiments were performed using the following cell lines: HEK293T, U87, human ATM$^{-/-}$and the corresponding isogenic ATM$^{+/+}$ controls, tet-on ATR^{KD}-expressing U2OS, immortal *Nfkb1*$^{+/+}$, *Nfkb1*$^{-/-}$ and *P65*$^{-/-}$ MEFs, and primary *Nfkb1*$^{+/+}$ and *Nfkb1*$^{-/-}$ MEFs, cultured as previously described.[20] Primary *Nfkb1*$^{+/+}$ and *Nfkb1*$^{-/-}$ MEFs were harvested at embryonic day 13.5. Stable re-expression of p50 isoforms was performed in *Nfkb1*$^{-/-}$ MEFs as previously described,[20] or using retroviral infection. Stable 293T-TopBP1^{ER} cells were constructed by selecting in puromycin following transfection with TopBP1^{ER}. *ATM*$^{+/+}$ and *ATM*$^{-/-}$ cells were purchased from Coriell Cell Repositories. The following siRNA constructs were obtained from Dharmacon: p50 (sense: GUCACUCUAACGUAUGCAAUU), ATR (M003202-05) and scrambled control (sense: CCUACGCCACCAAUUUCGUUU). Cells were transfected with siRNA using TransIT-TKO (Mirus) 24 hours prior to treatment or harvest for IB. U87 cells stably expressing sh-RNA targeting the C-terminal of p105, or control sequence, were previously described.[14]

For retroviral production, the pantropic platinum-GP retroviral packaging cell line (PlatGP) was transfected with retroviral vector containing various MigR1-p50 isoforms or TopBP1^{ER} using XtremeGENE transfection reagent (Roche). Target cells were then spinoculated with the virus/polybrene-containing supernatant. After infection, colonies were either sorted by FACS or selected in medium containing 0.5 μg/mL puromycin. Studies using *Nfkb1*$^{-/-}$ MEFs expressing p50 mutants represent data from at least 2 separate clones.

Poly(dA) $_{70}$-poly(dT) $_{70}$ oligos

TA oligos were obtained from IDT as poly(dA)$_{70}$ and poly (dT)$_{70}$ and pre-annealed prior to use. Studies in extracts were performed based on previous descriptions.[15,16] Briefly, nuclear extracts from immortal *Nfkb1*$^{-/-}$ MEFs were supplemented

with the indicated bacterially expressed p50 protein, purified as previously described,[14] and incubated with either single-stranded poly(dA)$_{70}$, or double-stranded poly(dA)$_{70}$-poly(dT)$_{70}$ oligonucleotides (25 pM) in kinase reaction buffer (50 mM Tris-HCl pH 7.5, 1 mM DTT, 10 mM $MgCl_2$, 10 mM $MnCl_2$,0.2 μM ATP) at 30°C for 1 hour. Reactions were then used for EMSA and immunoblotting. For *in vivo* studies, cells were transfected, using oligofectamine (Invitrogen), with the indicated concentration of oligo and EMSA or luciferase assay performed.

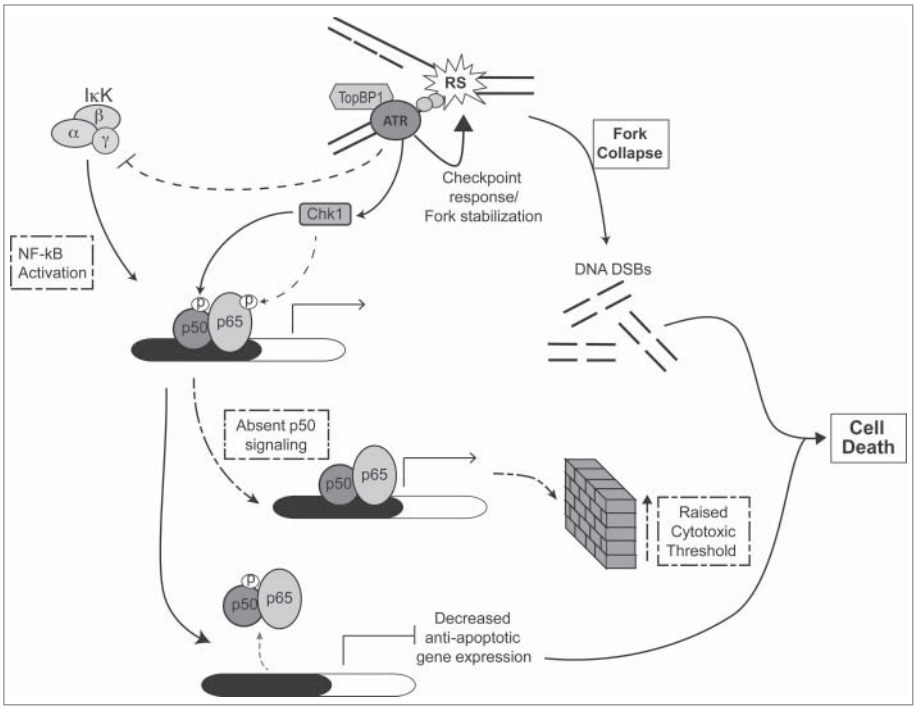

Figure 7. Model demonstrating role of p50 in the ATR-mediated response to RS. In this model, RS-induced ATR signaling leads to phosphorylation of nuclear p50 resulting in promoter-specific modulation of NF-κB (p50/p65) binding. This pathway, activated in parallel to the ATR-mediated checkpoint response, leads to attenuation of anti-apoptotic Bclxl expression. ATR signaling also modulates NF-κB activity by inhibiting the IκK complex and by inducing phosphorylation of p65. Together, the NF-κB-dependent response to ATR promotes cell death. Loss of p50 signaling leads to an elevation in the threshold for cell death resulting in survival of cells harboring higher levels of DNA strand breaks.

Synchronization and cell cycle analysis

Cell cycle analysis was made by evaluation of DNA content following incubation with propidium iodide (PI) as previously described.[41] For G2/M synchronization, cells were treated with 40 ng/ml nocodazole for 16 hours and then released. For thymidine synchronization, cells were grown in the presence of 2 mM thymidine (Sigma) for 16 hours, released for 8 hours into medium without thymidine and then re-incubated for 16 hours in thymidine. Harvested cells were then analyzed for cell cycle progression as above. For clonogenic assays in synchronized cells, cells were treated at the indicated time following release from thymidine block with 0.5 Gy IR. BrdU labeling was performed by pre-labeling cells with 10 μM BrdU for 60 minutes. Cells were then fixed and permeabilized according to the manufacturers' instructions (Cell Signaling). Flow cytometric analysis was performed after staining with anti-BrdU antibody (Santa Cruz, sc-32323).

Immunoprecipitation

Cells were treated as indicated and nuclear extracts prepared. IP was performed in buffer: [50 mM Tris (pH 8.), 125 mM NaCl, 1% Nonidet P-40 (NP-40), 10% glycerol and 2 mM EDTA] supplemented with 1 mM phenylmethylsulfonyl fluoride (PMSF). Extracts were pre-cleared with protein A/G conjugated Sepharose beads (GE Healthcare) and IP performed with the indicated antibodies and beads. Antigen-antibody complexes were precipitated with protein G beads and immunoblot performed following SDS-PAGE.

Luciferase reporter assay

Transfection was normalized using *renilla reniformis* and luciferase assay performed with the indicated NF-κB firefly reporter construct as previously described.[20] Data is plotted as firefly/*renilla* (F/R) relative luciferase. For luciferase assays with oligo substrates, cells were initially transfected with Ig-κB luciferase/*renilla* and 24 hours later treated with the indicated amount of oligo substrate in the presence of Oligofectamine (Invitrogen). Luciferase activity was quantified 6 hours after oligo administration. Assays were performed in triplicate at least thrice unless otherwise indicated.

Real time/quantitative reverse transcriptase (RT)-PCR

Total RNA was isolated from cells following treatment. The Protoscript M-MuLV Taq RT-PCR Kit (New England Biolabs) with poly-T primers was used for reverse transcriptase reaction. Transcripts were quantified using SYBR Green PCR (Bio-Rad), and normalized to *Gapdh* (mouse and human: sense 5′-CTTCACCACCATGGAGAAGGC-3′, antisense 5′-GGCATGGACTGTGGTCATGAG-3′). Primers included *Bclxl* (human: sense, 5′-GGTGAGTCGGATCGCAGC-3′; antisense, 5′-CAGCGGTTGAAGCGTTCC-3′; mouse: 5′-TTTGAATCCGCCACCATGTCTCAGAGCAACCGGGAGCTG-3′; antisense, 5′-TTTCTCGAGCTTTCCGACTGAAGAGTGAGCCCA-3′), *Bax* (sense, 5′-CCAGGATGCGTCCACCAAGAAG-3′, antisense, 5′-GGAGTCCGTGTCCACGTCAGC-3′). Data are averages of ≥ 3 independent experiments, each in triplicate.

Quantitative chromatin immunoprecipitation (qChIP)

Cells were left untreated or treated as indicated and IP performed with anti-p50, anti-Histone H1 or anti-mouse IgG to control for nonspecific binding. qPCR was performed with the *BCLXL* promoter specific primers: sense, 5′-GCACCACCTACATTCAAATCC-3′ and antisense, 5′-CGATGGAGGAGGAAGCAAGC-3′. Amplification was performed as described above and quantification of the change in DNA enrichment for each IP condition was determined relative to input DNA as previously described.[14]

Electrophoretic mobility shift assays (EMSA)

EMSA was performed following nuclear fraction isolation, or with purified protein, including treatment and supershift analysis as previously described.[14] A double-stranded oligonucleotide (5′-TCGAGTTAGATGGGGACTTTCCAGGCAC-3′) (IDT) containing the decameric κB-consensus sequence (underlined) was end labeled with [γ-^{32}P] ATP and used as a probe. Reaction mixtures were incubated at room temperature for 20 min prior to resolving on a 5% polyacrylamide gel (0.5x TBE) at ~10 V/cm for 2–4 hours at 4°C and assayed by autoradiography and PhosphorImager analysis (Molecular Dynamics). EMSA are representative of at least 3 independent experiments.

Clonogenic assays

Cells were plated and allowed to attach overnight. Following treatment, colony formation assay was performed as previously described.[14] The surviving fraction was calculated based on the plating efficiency of untreated cells.

γH2AX focus formation

Cells cultured on glass coverslips were fixed in 4% paraformaldehyde. Following permeabilization, cells were immunostained with phospho-S140-H2AX (Cell Signaling, 9718) and nuclei counterstained with 1 mg/ml 4',6-diamidino-2-phenylindole (DAPI) solution. Slides were imaged on a Zeiss microscope and the percentage of cells positive for γH2AX foci quantified in at least 200 cells per group.

Senescence associated (SA)-β-galactosidase staining

Primary MEFs at the indicated passage were plated onto 35 mm glass bottom plates (MatTek Corporation, Ashland, MA, USA) and at 60% confluency were fixed with formaldehyde for 20 minutes at 4°C. SA-β-galactosidase staining was performed in the standard fashion. Cells were incubated overnight with freshly made staining solution and the percentage of cells positive for SA-β-gal was calculated from a total of 200 cells per plate. Experiments were repeated in triplicate.

Metaphase spreads

Total breaks, gaps or constrictions on chromosomes were quantified on metaphase spreads stained by Giemsa (Sigma) essentially as previously described[42] but without aphidicolin pretreatment to obtain a homogeneous staining of chromosomes. Analysis of samples was made in a blinded fashion by 2 independent observers.

Single-cell gel electrophoresis (comet) assay

Alkaline comet assay was performed as described previously.[43] Nuclei were visualized on a Zeiss microscope and images analyzed with ImageJ (NIH). DNA damage was quantified for 50 cells by determining the percentage of the cellular DNA within the tail using Comet Score (TriTek).

Homologous recombination analysis

The assay was performed essentially as described.[44] HEK293 cells stably expressing the recombination substrate, DR-GFP, were a generous gift from Dr. from Phillip Connell and were grown to 70% confluence prior to transfection with p50 or scrambled siRNA. Cells were grown in complete growth medium for 24 hours and then re-transfected with the I-SceI expression vector, pCβASce, or the control vector, pCAGGS. Cells were incubated for an additional 24 hours in normal medium and then analyzed with a Becton-Dickinson FACScan. Alternatively, *Nfkb1*$^{-/-}$ MEFs stably expressing p50^{WT}, p50^{S329A} or empty vector were co-transfected with the pHR-DR-GFP reporter vector and either pCβASce or pCAGGS. Cells were grown in complete growth medium for 24 hours in normal medium and then analyzed with a Becton-Dickinson FACScan. For HR analysis, live cells were collected based on size/complexity and propidium iodide (PtdIns) exclusion and the fraction of live cells exhibiting GFP positivity displayed ± SEM of triplicate samples repeated.

Statistical analysis

Statistical analyses were performed using a 2-tailed Student's *t*-test.

Disclosure of Potential Conflicts of Interest

No potential conflicts of interest were disclosed.

Acknowledgments

We are grateful to Oscar Fernandez-Capetillo, Warner Greene and Phillip Connell for plasmids, P. Nghiem for tet-on U2OS cells, Elizabeth Davis for assistance with metaphase spreads and Adam Schmitt for critical reading of the manuscript.

Funding

This work was supported by National Institutes of Health (NIH) grant R01CA136937 to B.Y. and the Ludwig Center for Metastasis Research.

Supplemental Material

Supplemental data for this article can be accessed on the publisher's website.

References

1. Lopez-Contreras AJ, Fernandez-Capetillo O. The ATR barrier to replication-born DNA damage. DNA Repair (Amst) 2010; 9: 1249-55; PMID:21036674
2. Garner E, Costanzo V. Studying the DNA damage response using in vitro model systems. DNA Repair (Amst) 2009; 8: 1025-37; PMID:19482562
3. Cimprich KA, Cortez D. ATR: an essential regulator of genome integrity. Nat Rev Mol Cell Biol 2008; 9: 616–27; PMID:18594563; http://dx.doi.org/10.1038/nrm2450
4. Kumagai A, Lee J, Yoo HY, Dunphy WG. TopBP1 activates the ATR-ATRIP complex. Cell 2006; 124: 943-55; PMID:16530042; http://dx.doi.org/10.1016/j.cell.2005.12.041
5. Toledo LI, Murga M, Gutierrez-Martinez P, Soria R, Fernandez-Capetillo O. ATR signaling can drive cells into senescence in the absence of DNA breaks. Genes Dev 2008; 22: 297-302; PMID:18245444; http://dx.doi.org/10.1101/gad.452308
6. Brown EJ, Baltimore D. Essential and dispensable roles of ATR in cell cycle arrest and genome maintenance. Genes Dev 2003; 17: 615-28; PMID:12629044; http://dx.doi.org/10.1101/gad.1067403
7. Rothkamm K, Lobrich M. Evidence for a lack of DNA double-strand break repair in human cells exposed to very low x-ray doses. Proc Natl Acad Sci U S A 2003; 100: 5057-62; PMID:12679524; http://dx.doi.org/10.1073/pnas.0830918100
8. Janssens S, Tschopp J. Signals from within: the DNA-damage-induced NF-kappaB response. Cell Death Differ 2006; 13: 773-84; PMID:16410802; http://dx.doi.org/10.1038/sj.cdd.4401843
9. Wu ZH, Shi Y, Tibbetts RS, Miyamoto S. Molecular linkage between the kinase ATM and NF-kappaB signaling in response to genotoxic stimuli. Science 2006; 311: 1141-6; PMID:16497931; http://dx.doi.org/10.1126/science.1121513
10. Wu ZH, Miyamoto S. Induction of a pro-apoptotic ATM-NF-kappaB pathway and its repression by ATR in response to replication stress. Embo J 2008; 27: 1963-73; PMID:18583959; http://dx.doi.org/10.1038/emboj.2008.127
11. Rocha S, Campbell KJ, Perkins ND. p53- and Mdm2-independent repression of NF-kappa B transactivation by the ARF tumor suppressor. Mol Cell 2003; 12: 15-25; PMID:12887889; http://dx.doi.org/10.1016/S1097-2765(03)00223-5
12. Hayden MS, Ghosh S. NF-kappaB, the first quarter-century: remarkable progress and outstanding questions. Genes Dev 2012; 26: 203-34; PMID:22302935; http://dx.doi.org/10.1101/gad.183434.111
13. Barre B, Perkins ND. A cell cycle regulatory network controlling NF-kappaB subunit activity and function. Embo J 2007; 26: 4841-55; PMID:17962807; http://dx.doi.org/10.1038/sj.emboj.7601899
14. Schmitt AM, Crawley CD, Kang S, Raleigh DR, Yu X, Wahlstrom JS, Voce DJ, Darga TE, Weichselbaum RR, Yamini B. p50 (NF-kappaB1) is an effector protein in the cytotoxic response to DNA methylation damage. Mol Cell 2011; 44: 785-96; PMID:22152481; http://dx.doi.org/10.1016/j.molcel.2011.09.026
15. Kumagai A, Dunphy WG. Claspin, a novel protein required for the activation of Chk1 during a DNA replication checkpoint response in Xenopus egg extracts. Mol Cell 2000; 6: 839-49; PMID:11090622; http://dx.doi.org/10.1016/S1097-2765(05)00092-4
16. Clarke CA, Clarke PR. DNA-dependent phosphorylation of Chk1 and Claspin in a human cell-free system. Biochem J 2005; 388: 705-12; PMID:15707391; http://dx.doi.org/10.1042/BJ20041966
17. Nghiem P, Park PK, Ys Kim YS, Desai BN, Schreiber SL. ATR is not required for p53 activation but synergizes with p53 in the replication checkpoint. J Biol Chem 2002; 277: 4428-34; PMID:11711532; http://dx.doi.org/10.1074/jbc.M106113200
18. Zou L. Single- and double-stranded DNA: building a trigger of ATR-mediated DNA damage response. Genes Dev 2007; 21: 879-85; PMID:17437994; http://dx.doi.org/10.1101/gad.1550307
19. Crawley CD, Raleigh DR, Kang S, Voce DJ, Schmitt AM, Weichselbaum RR, Yamini B. DNA damage-induced cytotoxicity is mediated by the cooperative interaction of phospho-NF-kappaB p50 and a single nucleotide in the kappaB-site. Nucleic Acids Res 2013; 41: 764-74; PMID:23180782; http://dx.doi.org/10.1093/nar/gks1120
20. Yamini B, Yu X, Dolan ME, Wu MH, Darga TE, Kufe DW, Weichselbaum RR. Inhibition of nuclear factor-kappaB activity by temozolomide involves O6-methylguanine induced inhibition of p65 DNA binding. Cancer Res 2007; 67: 6889-98; PMID:17638900; http://dx.doi.org/10.1158/0008-5472.CAN-06-4496
21. Hekmat-Nejad M, You Z, Yee MC, Newport JW, Cimprich KA. Xenopus ATR is a replication-dependent chromatin-binding protein required for the DNA replication checkpoint. Curr Biol 2000; 10: 1565-73; PMID:11137007; http://dx.doi.org/10.1016/S0960-9822(00)00855-1
22. Dart DA, Adams KE, Akerman I, Lakin ND. Recruitment of the cell cycle checkpoint kinase ATR to chromatin during S-phase. J Biol Chem 2004; 279: 16433-40; PMID:14871897; http://dx.doi.org/10.1074/jbc.M314212200
23. Arnaudeau C, Lundin C, Helleday T. DNA double-strand breaks associated with replication forks are predominantly repaired by homologous recombination involving an exchange mechanism in mammalian cells. J Mol Biol 2001; 307: 1235-45; PMID:11292338; http://dx.doi.org/10.1006/jmbi.2001.4564
24. Kuilman T, Michaloglou C, Mooi WJ, Peeper DS. The essence of senescence. Genes Dev 2010; 24: 2463-79; PMID:21078816; http://dx.doi.org/10.1101/gad.1971610
25. Hoffmann A, Leung TH, Baltimore D. Genetic analysis of NF-kappaB/Rel transcription factors defines functional specificities. Embo J 2003; 22: 5530-9; PMID:14532125; http://dx.doi.org/10.1093/emboj/cdg534
26. Shechter D, Costanzo V, Gautier J. Regulation of DNA replication by ATR: signaling in response to DNA intermediates. DNA Repair (Amst) 2004; 3: 901-8; PMID:15279775
27. Flynn RL, Zou L. ATR: a master conductor of cellular responses to DNA replication stress. Trends Biochem Sci 2011; 36: 133-40; PMID:20947357; http://dx.doi.org/10.1016/j.tibs.2010.09.005
28. Brown EJ, Baltimore D. ATR disruption leads to chromosomal fragmentation and early embryonic lethality. Genes Dev 2000; 14: 397-402; PMID:10691732
29. de Klein A, Muijtjens M, van Os R, Verhoeven Y, Smit B, Carr AM, Lehmann AR, Hoeijmakers JH. Targeted disruption of the cell-cycle checkpoint gene ATR leads to early embryonic lethality in mice. Curr Biol 2000; 10: 479-82; PMID:10801416; http://dx.doi.org/10.1016/S0960-9822(00)00447-4
30. Cortez D, Guntuku S, Qin J, Elledge SJ. ATR and ATRIP: partners in checkpoint signaling. Science 2001; 294: 1713-6; PMID:11721054; http://dx.doi.org/10.1126/science.1065521
31. Nghiem P, Park PK, Kim Y, Vaziri C, Schreiber SL. ATR inhibition selectively sensitizes G1 checkpoint-deficient cells to lethal premature chromatin condensation. Proc Natl Acad Sci U S A 2001; 98: 9092-7; PMID:11481475; http://dx.doi.org/10.1073/pnas.161281798
32. Abraham RT. Cell cycle checkpoint signaling through the ATM and ATR kinases. Genes Dev 2001; 15: 2177-96; PMID:11544175
33. Tercero JA, Longhese MP, Diffley JF. A central role for DNA replication forks in checkpoint activation and response. Mol Cell 2003; 11: 1323-36; PMID:12769855; http://dx.doi.org/10.1016/S1097-2765(03)00169-2
34. Desany BA, Alcasabas AA, Bachant JB, Elledge SJ. Recovery from DNA replicational stress is the essential function of the S-phase checkpoint pathway. Genes Dev 1998; 12: 2956-70; PMID:9744871; http://dx.doi.org/10.1101/gad.12.18.2956
35. Branzei D, Foiani M. The checkpoint response to replication stress. DNA Repair (Amst) 2009; 8: 1038-46; PMID:19482564
36. Malkova A, Haber JE. Mutations arising during repair of chromosome breaks. Annu Rev Genet 2012; 46: 455-73; PMID:23146099; http://dx.doi.org/10.1146/annurev-genet-110711-155547
37. Sha WC, Liou HC, Tuomanen EI, Baltimore D. Targeted disruption of the p50 subunit of NF-kappa B leads to multifocal defects in immune responses. Cell 1995; 80: 321-30; PMID:7834752; http://dx.doi.org/10.1016/0092-8674(95)90415-8
38. Lu ZY, Yu SP, Wei JF, Wei L. Age-related neural degeneration in nuclear-factor kappaB p50 knockout mice. Neuroscience 2006; 139: 965-78; PMID:16533569; http://dx.doi.org/10.1016/j.neuroscience.2005.12.062
39. Fullard N, Moles A, O'Reilly S, van Laar JM, Faini D, Diboll J, Reynolds NJ, Mann DA, Reichelt J, Oakley F. The c-Rel subunit of NF-kappaB regulates epidermal homeostasis and promotes skin fibrosis in mice. Am J Pathol 2013; 182: 2109-20; PMID:23562440; http://dx.doi.org/10.1016/j.ajpath.2013.02.016
40. Denis-Donini S, Dellarole A, Crociara P, Francese MT, Bortolotto V, Quadrato G, Canonico PL, Orsetti M, Ghi P, Memo M, et al. Impaired adult neurogenesis associated with short-term memory defects in NF-kappaB p50-deficient mice. The Journal of neuroscience : the official journal of the Society for Neuroscience 2008; 28: 3911-9; PMID:18400889; http://dx.doi.org/10.1523/JNEUROSCI.0148-08.2008
41. Yamini B, Yu X, Gillespie GY, Kufe DW, Weichselbaum RR. Transcriptional targeting of adenovirally delivered tumor necrosis factor alpha by temozolomide in experimental glioblastoma. Cancer Res 2004; 64: 6381-4; PMID:15374943; http://dx.doi.org/10.1158/0008-5472.CAN-04-2117
42. Glover TW, Berger C, Coyle J, Echo B. DNA polymerase alpha inhibition by aphidicolin induces gaps and breaks at common fragile sites in human chromosomes. Hum Genet 1984; 67: 136-42; PMID:6430783; http://dx.doi.org/10.1007/BF00272988
43. Singh NP, McCoy MT, Tice RR, Schneider EL. A simple technique for quantitation of low levels of DNA damage in individual cells. Exp Cell Res 1988; 175: 184-91; PMID:3345800; http://dx.doi.org/10.1016/0014-4827(88)90265-0
44. Pierce AJ, Johnson RD, Thompson LH, Jasin M. XRCC3 promotes homology-directed repair of DNA damage in mammalian cells. Genes Dev 1999; 13: 2633-8; PMID:10541549; http://dx.doi.org/10.1101/gad.13.20.2633